MDPI

Article

InGaN Based C-Plane Blue Laser Diodes on Strain Relaxed Template with Reduced Absorption Loss

Hsun-Ming Chang [1,*], Philip Chan [1], Norleakvisoth Lim [2], Vincent Rienzi [3], Haojun Zhang [1], Daniel A. Cohen [3], Michael J. Gordon [2], Steven P. DenBaars [1,3] and Shuji Nakamura [1,3]

[1] Department of Electrical and Computer Engineering, University of California, Santa Barbara, CA 93106, USA
[2] Department of Chemical Engineering, University of California, Santa Barbara, CA 93106, USA
[3] Materials Department, University of California, Santa Barbara, CA 93106, USA
* Correspondence: hsun-ming@ucsb.edu

Abstract: InGaN based c-plane blue LDs on strain relaxed template (SRT) with a reduced absorption loss was demonstrated. The loss is reduced from 27 cm^{-1} to 20 cm^{-1}. Due to the lower loss, threshold current density is improved from 51.1 kA/cm^2 to 43.7 kA/cm^2, and slope efficiency is also increased by a factor of 1.22. The absorption loss from decomposition layer (DL) in SRT is confirmed to be a major extra loss source by both experimental and simulation results. With a higher indium content in buffer and waveguide layers, optical leakage into DL can be suppressed.

Keywords: III-nitrides; laser diodes; strain relaxed template; optical loss

Citation: Chang, H.-M.; Chan, P.; Lim, N.; Rienzi, V.; Zhang, H.; Cohen, D.A.; Gordon, M.J.; DenBaars, S.P.; Nakamura, S. InGaN Based C-Plane Blue Laser Diodes on Strain Relaxed Template with Reduced Absorption Loss. *Crystals* **2022**, *12*, 1230. https://doi.org/10.3390/cryst12091230

Received: 3 August 2022
Accepted: 29 August 2022
Published: 1 September 2022

Publisher's Note: MDPI stays neutral with regard to jurisdictional claims in published maps and institutional affiliations.

Copyright: © 2022 by the authors. Licensee MDPI, Basel, Switzerland. This article is an open access article distributed under the terms and conditions of the Creative Commons Attribution (CC BY) license (https://creativecommons.org/licenses/by/4.0/).

1. Introduction

Visible laser diodes (LDs) are promising for next-generation display applications such as VR/AR, head-up display, and pico-projectors [1]. While AlGaInP based LDs have been realized for red light source, InGaN based LDs are advantageous in blue and green [2–4]. Although efficient blue InGaN LDs are well developed, green LDs with a comparable performance to blue remains challenging, which is also known as the "green gap" [5]. Extending wavelength to green causes an increased strain in InGaN layer due to the 10% lattice mismatch between GaN and InN, resulting in deterioration of material quality such as composition pulling effect and phase separation [6–10]. Besides, because of the piezoelectricity of III-Nitrides, quantum-confined Stark effect (QCSE) will exacerbate due to the higher strain in green, causing an increase in electron-hole wavefunction separation and thus degrading the optical gain for LDs [10–12].

To deal with these issues, ideas of relieving the strain in InGaN layer have been proposed. A relaxed InGaN layer can not only tackle the problems mentioned above, but also enable higher indium (In) incorporation, and thus a higher growth temperature with superior material quality can be potentially achieved. So far, several methods have been reported, including semi-relaxed InGaN substrates and porous GaN pseudo-substrates [13–18]. However, most of these methods require complicated processing such as patterning, wafer bonding and regrowth, which is not favorable in manufacturing perspectives. Recently, P. Chan et al. demonstrated a simple strain relaxed template (SRT) without any regrowth or patterning or wafer bonding, and more than 85% biaxial relaxation of the InGaN buffer layer above has been realized as well as decent red LEDs results [19–21]. In addition, blue LDs have also been achieved on SRT recently [22]. However, a significantly higher loss was found in SRT LDs, and the source of it is unclear yet.

In this work, we successfully demonstrate InGaN based LDs grown on SRT with a lower internal loss. From segmented contact measurement, the loss is reduced from 27 cm^{-1} to 20 cm^{-1}. Due to a lower loss, threshold current density is improved from 51.1 kA/cm^2 to 43.7 kA/cm^2, and slope efficiency is also increased by a factor of 1.22. Transmission measurement and 1D optical mode simulation was done to verify the loss source. It is

realized that a significant amount of loss is generated from mode leakage into the highly light absorbing decomposition layer (DL) in SRT. By optimizing the waveguide/cladding structure to minimize the optical mode leakage, it is promising to reduce the loss of SRT LDs to a similar amount as those without SRT.

2. Materials and Methods

The LD epi was grown by metal−organic chemical vapor deposition (MOCVD) on freestanding bulk c-plane substrates instead of sapphire to minimize threading dislocation density [23]. Two different epi designs denoted as SRT1 and SRT2 were grown with different In content in buffer and waveguide, while all other layers were kept the same for fair comparison. As shown in Figure 1, the epi started with a 2.6 µm n-GaN template growth, followed by the growth of SRT which consisted of a 3 nm InGaN DL grown at 750 °C, and a 700 nm n-GaN decomposition stop layer (DSL) at 1100 °C which also served as n-cladding layer. After that, a 100 nm of n-InGaN/GaN superlattices (SLs) were grown as buffer layer consisting of 5 periods of 16 nm InGaN and 4 nm GaN, where the average In composition is denoted as “x” and the number corresponds to the sample number. The buffer layer was grown under low ammonia flow to increase Ga adatom mobility and thus suppress the formation of V-pits [24]. Then, a 60 nm InGaN waveguide was grown, with the In composition denoted as “y” and the number corresponds to the sample number. After that, active region composed of a 4 periods quantum wells of 2.5 nm InGaN, 2 nm AlGaN (11% Al) and 9 nm of GaN was grown. The In content is estimated as 18–19% for SRT1 and 20–21% for SRT2. And then a 10 nm of p-AlGaN (11% Al) was grown as electron blocking layer (EBL), followed by the same waveguide structure in p-side, a 210 nm of p-GaN as p-cladding and 15 nm of p + GaN as p-contact layer. After the epi growth, high resolution x-ray diffraction (HRXRD) reciprocal space map (RSM) was conducted to analyze the relaxation and In content of InGaN buffer and waveguide of both epi designs using $(\overline{1}\overline{1}24)$ as off-axis.

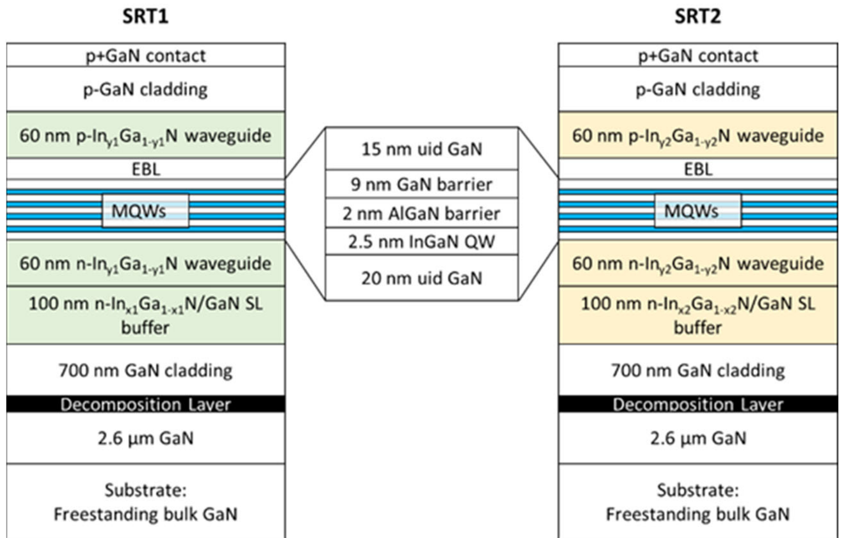

Figure 1. Schematic of the SRT LD epitaxial design. Indium composition in buffer and waveguide is denoted as x, y, and the numbers correspond to SRT1 or SRT2, respectively.

Ridge stripe laser structures are used in this work. The process started with ridge etching by reactive-ion-etching (RIE) followed by a self-aligned liftoff SiO_2 deposition and liftoff process. After that, Indium Tin Oxide (ITO) was deposited as p-contact and cladding layer, which enabled thinner p-GaN cladding and therefore a better operating voltage [25]. A Ti/Au metal stack was then deposited as metal pad for probing. Finally, both facets were formed by chemically assisted ion beam etching (CAIBE) with an Ar ion beam in a Cl_2

atmosphere [26], and backside Ti/Al/Ni/Au metal was deposited as n-electrode. Both devices were fabricated together to avoid variation in processing conditions.

The fabricated LDs were tested under pulse mode using a pulse generator with a pulse width of 500 ns and a duty cycle of 0.5%. Electroluminescence (EL) spectrum was collected by an optical fiber connected to Ocean-Optics spectrometer, and the light output power was measured by integrating sphere. Segmented contact method was carried out to measure the optical loss utilizing the amplified spontaneous emission (ASE) spectra, where the method and principles can be found in [27,28].

To understand the optical loss in the current LD structure, transmission measurement and 1D optical mode simulation were done. A reflectometer (model: F10−RT−UVX by Filmetrics) at UCSB Nanofab was used to measure the transmission and absorption coefficient of DL. Two samples were grown on double side polished (DSP) sapphire for the measurement: one without DL as baseline and the other one with DL. The growths started with a low temperature (LT) GaN as nucleation layer and then a high temperature (HT) thick GaN growth for film to coalesce. After that, the same DL as laser samples was grown, while for the baseline sample the In flow was removed so a thin LT GaN was grown instead. And then, the temperature was raised to 1100 °C to grow a 400 nm GaN and decompose DL. The transmission of DL was then measured with the baseline sample as a reference, and the absorption coefficient can be extracted from the transmission based on Beer-Lambert's law: $T = e^{-\langle \alpha_{DL} \rangle t_{DL}}$, where T is the transmission, $\langle \alpha_{DL} \rangle$ is the absorption coefficient of DL and t_{DL} is the thickness of DL.

1D mode simulation was done by our home-made Matlab code using transfer matrix method. Details of the simulation such as the model used to calculate refractive indices and absorption coefficient numbers can be found in [29]. LD structures of both samples are set to be the same as the sample epi mentioned in above paragraph, where the In composition used in InGaN buffer and waveguide was obtained from RSM results.

3. Results and Discussion

RSM results of SRT1 and SRT2 from HRXRD are shown in Figure 2. From the peak intensity and position of InGaN and GaN, we can obtain the In composition as the followings: x1 = 0.029, y1 = 0.05, x2 = 0.033, y2 = 0.063. For SRT1, the InGaN buffer is 46.9% relaxed and waveguide is 36.7% relaxed, while for SRT2, the InGaN buffer is 61.9% relaxed and the waveguide is 40.7% relaxed, with a calculation error range of 3–5%. Note that a strong peak on the left side of the GaN substrate peak is observed for both samples, which corresponds to the 700 nm GaN cladding layer under tensile strain according to peak intensity and position. Although not shown here, we found the tensile GaN peak existed even without any InGaN layer grown on top, suggesting that the tensile strain arises from some defects forming during GaN growth on DL. Although more experiments and characterizations are required, it is postulated that inclined threading dislocations could be the possible reason [30], which has already been reported to be the mechanism of tensile strain in AlGaN grown on AlGaN buffer/sapphire [31–33]. As can be observed, the GaN cladding of SRT2 is under a higher degree of tensile strain, meaning a larger in-plane lattice constant. Hence, the lattice mismatch of the InGaN layers grown on top is reduced, leading to a higher relaxation degree and In content. Although the relaxation is not high compared to our previous work of more than 85%, the 700 nm high temperature GaN help prevent morphology degradation as mentioned in [22].

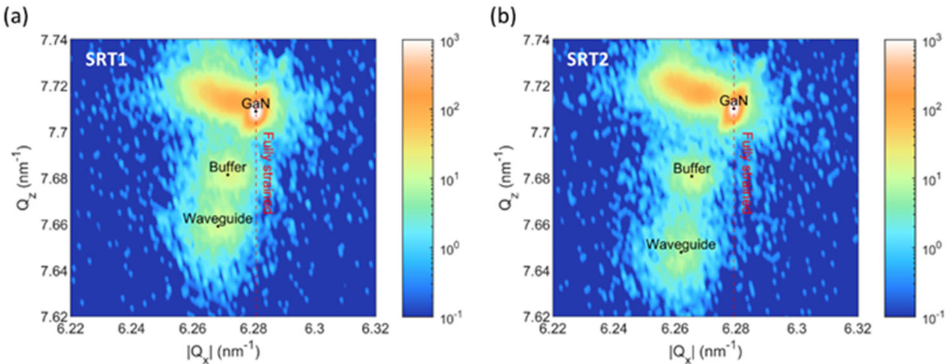

Figure 2. RSM results of (**a**) SRT1 and (**b**) SRT2 from HRXRD utilizing $\left(\overline{1}\overline{1}24\right)$ off-axis.

The EL spectrum and single-facet light–current (L–I) characteristics of the ridge with 1800 µm cavity length and 1.5 µm ridge width are shown in Figure 3a,b. The LDs show a narrow lasing peak at 460.5 nm and 465.29 nm for SRT1 and SRT2, respectively. From the L-I curve we can obtain the threshold current density (J_{th}) of 51.1 kA/cm^2 and 43.7 kA/cm^2 for SRT1 and SRT2, respectively. Segmented contact measurement results of SRT1 and SRT2 are also shown in Figure 4. To have a fair comparison, the same ridge width (1.5 µm) was measured for both structures. From the measurement, one can get the spectra of $\Gamma g - \langle \alpha_i \rangle$ and $-\Gamma \alpha - \langle \alpha_i \rangle$ under various injection current, where Γ is the confinement factor, g stands for gain, α stands for absorption and $\langle \alpha_i \rangle$ is the internal loss. The internal loss $\langle \alpha_i \rangle$ can be extracted at long wavelength range where there is no absorption from the active region, which is 27 cm^{-1} and 20 cm^{-1} for SRT1 and SRT2, respectively. It is also important to note that the slope efficiency extracted from L-I characteristics is 0.0249 W/A for SRT1 and 0.0296 W/A for SRT2. Under a reasonable assumption that the carrier injection efficiency and mirror loss is the same for both samples, slope efficiency is then only dependent on $\langle \alpha_i \rangle$ [34]. Therefore, the observed higher slope efficiency confirms the lower loss in SRT2, which is also as expected since J_{th} of SRT2 is lower. It worth noting that the slope efficiency is very poor compared to other work. Besides the high loss, we found that the poor injection efficiency (η_i) in our LD design is even more detrimental to the low slope efficiency: although not shown here, the LDs without SRT has a η_i of only around 27%. With a higher loss of SRT, the devices need to be pumped even harder to reach threshold, resulting in more bending in band diagram and thus more carriers leaking out from active region. Assuming a perfect GaN/air interface, the mirror loss can be calculated as 10 cm^{-1} for an 1800 µm cavity [34]. Using the above loss numbers, the calculated η_i is only 9% for SRT LDs, which is not surprising considering their high threshold.

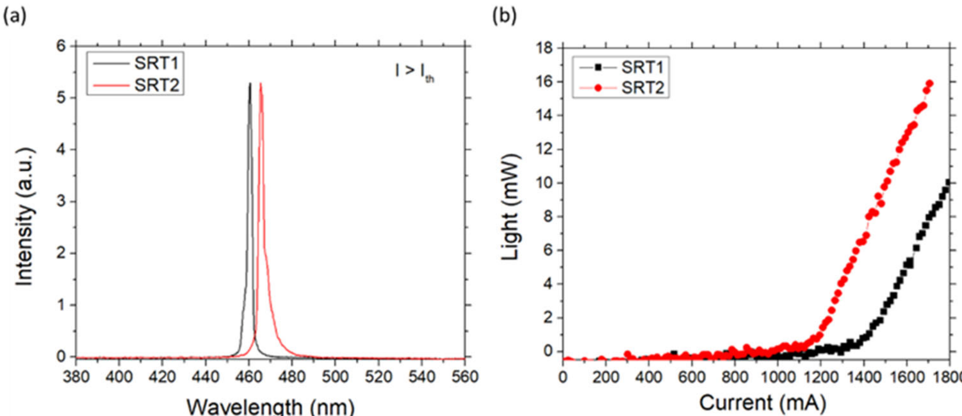

Figure 3. (**a**) EL spectrum showing the lasing peak at 460.5 and 465.29 nm for SRT1 and SRT2, respectively. (**b**) Single facet L-I characteristics of SRT1 and SRT2.

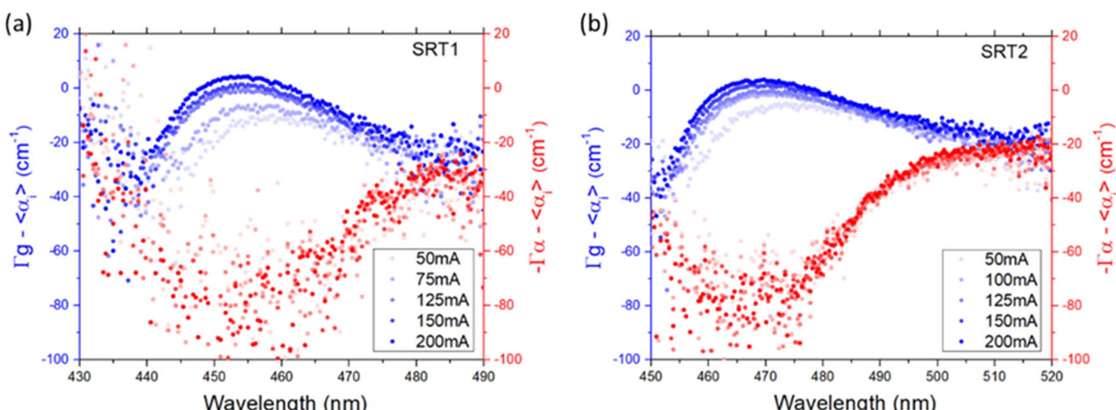

Figure 4. Gain and loss spectra of (**a**) SRT1 and (**b**) SRT2 from segmented contact measurement.

The measured absorption coefficient $\langle\alpha_{DL}\rangle$ from transmission measurement was 6×10^4–8×10^4 cm^{-1} in a wavelength range of 455–470 nm although not shown here. By multiplying the simulated confinement factor in DL (Γ_{DL}) and $\langle\alpha_{DL}\rangle$, absorption loss of DL (α_{DL}) can be calculated. The simulation results are summarized in Table 1. As shown in the table, τ_{DL} of SRT2 is reduced to almost a half compared to SRT1, and α_{DL} is 31 cm^{-1} and 18.1 cm^{-1} for SRT1 and SRT2, respectively. As expected, absorption loss from all other layers beside DL ($\alpha_{all\ others}$) for both SRT1 and SRT2 is close to 10 cm^{-1}, which agrees well with the loss of LDs without SRT in [22]. Absorption loss from DL can also be estimated from segmented contact measurement results if we assume the extra loss of SRT LDs all comes from DL absorption and all other layers have the same total absorption of 10 cm^{-1}. In this case, the estimated α_{DL} for SRT1 and SRT2 is 17 cm^{-1} and 10 cm^{-1}, respectively. Note that although the deviation between experimental and simulation results could be large due to an unknown refractive index in active region and DL, the trend of the loss values agrees well between them: when comparing SRT1 to SRT2, α_{total} from simulation reduced by a factor of 0.747, which is almost equal to the number (0.741) obtained from segmented contact measurement.

Table 1. Summary of 1D mode simulation results between SRT1 and SRT2, and the structure "New" with better optimized waveguide/cladding structure.

	Γ_{MQWs} (%)	Γ_{DL} (%)	α_{DL} (cm^{-1})	$\alpha_{all\ others}$ (cm^{-1})	α_{total} (cm^{-1})
SRT1	2.21	5.10×10^{-2}	31.0	9.28	40.3
SRT2	2.43	2.65×10^{-2}	18.1	11.98	30.1
New	2.42	3.96×10^{-4}	0.27	12.812	13.1

From the above results, absorption from DL can therefore be confirmed as the major source of extra loss. The physics behind the loss reduction in SRT2 is because of a higher In content in buffer and waveguide which suppresses optical leakage into DL as can be seen in the simulation results as well. Note that the confinement factor difference in MQWs (Γ_{MQWs}) for both devices is not remarkable compared to the loss, so it is again confirmed that the improvement of J_{th} and slope efficiency is mainly due to the lower loss of SRT2. By optimizing the waveguide/cladding design, it is promising to approach an even lower loss close to LDs without SRT. A more optimized LD structure denoted as "New" was simulated, where the epi is same as SRT2 but with 100 nm of InGaN waveguide and 1 µm of n-GaN cladding. Both thicker waveguide and cladding thickness can reduce the mode leakage. As shown in Table 1, the mode leakage can be greatly suppressed to less than 1 cm^{-1}, which is almost negligible compared to the total loss of LD without SRT. The simulated mode profile is shown in Figure 5, where there is little E-field leakage into DL as expected.

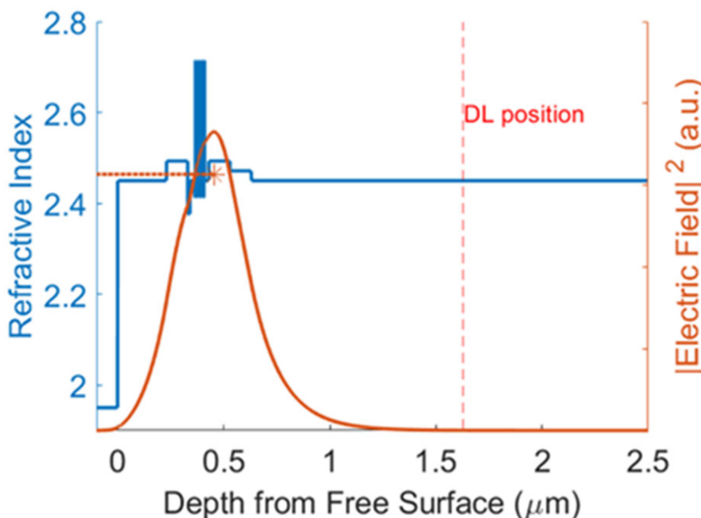

Figure 5. 1D mode simulation of the New SRT structure as listed in Table 1.

4. Conclusions

In conclusions, InGaN based LDs grown on SRT with a lower internal loss and a lower J_{th} are demonstrated. From segmented contact measurement, the loss is reduced from 27 cm^{-1} to 20 cm^{-1}, and J_{th} is improved from 51.1 kA/cm^2 to 43.7 kA/cm^2, with a 1.22 times improvement in slope efficiency. Transmission measurement and 1D optical mode simulation was done to verify the loss source. It is identified that a significant amount of loss is generated from the mode leakage into the highly light absorbing decomposition layer in SRT. By optimizing the waveguide/cladding structure to minimize the optical mode leakage, it is promising to reduce the loss of SRT LDs to a similar amount as those without SRT.

Author Contributions: Formal analysis, H.-M.C.; investigation, H.-M.C.; data curation, H.-M.C. and P.C.; software, P.C., N.L. and H.-M.C.; writing—original draft preparation, H.-M.C.; writing—review and editing, P.C., N.L., V.R., H.Z. and D.A.C.; visualization, H.-M.C.; supervision, S.N., S.P.D. and M.J.G.; project administration, S.N., S.P.D. and M.J.G.; funding acquisition, S.N., S.P.D. and M.J.G. All authors have read and agreed to the published version of the manuscript.

Funding: This work was funded by Google under Grant No. PO4100162358 and the Defense Advanced Research Projects Agency (DARPA) under Grant No. HR001120C0135. The results presented made use of the MRL Shared Experimental Facilities of UCSB supported by the MRSEC program (NSF DMR 1720256), a member of the Materials Research Facilities Network (www.mrfn.org, accessed on 30 April 2021), as well as the UCSB Nanofabrication Facility, an open access laboratory.

Data Availability Statement: Results presented in this paper are not available publicly at this time but may be obtained from the authors upon reasonable request.

Conflicts of Interest: The authors declare no conflict of interest.

References

1. Hardy, M.T.; Feezell, D.F.; Denbaars, S.; Nakamura, S. Group III-nitride lasers: A materials perspective. *Mater. Today* **2011**, *14*, 408–415. [CrossRef]
2. Nakamura, S.; Senoh, M.; Nagahama, S.-i.; Iwasa, N.; Matsushita, T.; Mukai, T. Blue InGaN-based laser diodes with an emission wavelength of 450 nm. *Appl. Phys. Lett.* **2000**, *76*, 22–24. [CrossRef]
3. Yoshizumi, Y.; Adachi, M.; Enya, Y.; Kyono, T.; Tokuyama, S.; Sumitomo, T.; Akita, K.; Ikegami, T.; Ueno, M.; Katayama, K.; et al. Continuous-wave operation of 520 nm green InGaN-based laser diodes on semi-polar {2021} GaN substrates. *Appl. Phys. Express* **2009**, *2*, 092101. [CrossRef]
4. Nakatsu, Y.; Nagao, Y.; Kozuru, K.; Hirao, T.; Okahisa, E.; Masui, S.; Yanamoto, T.; Nagahama, S.-I. High-efficiency blue and green laser diodes for laser displays. In *Gallium Nitride Materials and Devices XIV*; SPIE: Bellingham, WA, USA, 2019; Volume 10918, pp. 99–107.
5. der Maur, M.A.; Pecchia, A.; Penazzi, G.; Rodrigues, W.; di Carlo, A. Efficiency drop in green InGaN/GaN light emitting diodes: The role of random alloy fluctuations. *Phys. Rev. Lett.* **2016**, *116*, 027401. [CrossRef]

6. Pereira, S.; Correia, M.R.; Pereira, E.; O'donnell, K.P.; Trager-Cowan, C.; Sweeney, F.; Alves, E. Compositional pulling effects in In x Ga 1-x N/G a N layers: A combined depth-resolved cathodoluminescence and Rutherford backscattering/channeling study. *Phys. Rev. B* **2001**, *64*, 205311. [CrossRef]
7. McCluskey, M.D.; Romano, L.T.; Krusor, B.S.; Bour, D.P.; Johnson, N.M.; Brennan, S. Phase separation in InGaN/GaN multiple quantum wells. *Appl. Phys. Lett.* **1998**, *72*, 1730–1732. [CrossRef]
8. Hiramatsu, K.; Kawaguchi, Y.; Shimizu, M.; Sawaki, N.; Zheleva, T.; Davis, R.; Tsuda, H.; Taki, W.; Kuwano, N.; Oki, K. The composition pulling effect in MOVPE grown InGaN on GaN and AlGaN and its TEM characterization. *MRS Internet J. Nitride Semicond. Res.* **1997**, *2*, 1–12. [CrossRef]
9. El-Masry, N.A.; Piner, E.L.; Liu, S.X.; Bedair, S.M. Phase separation in InGaN grown by metalorganic chemical vapor deposition. *Appl. Phys. Lett.* **1998**, *72*, 40–42. [CrossRef]
10. Bykhovski, A.D.; Gelmont, B.L.; Shur, M.S. Elastic strain relaxation and piezoeffect in GaN-AlN, GaN-AlGaN and GaN-InGaN superlattices. *J. Appl. Phys.* **1997**, *81*, 6332–6338. [CrossRef]
11. Scheibenzuber, W.G.; Schwarz, U.T.; Veprek, R.G.; Witzigmann, B.; Hangleiter, A. Calculation of optical eigenmodes and gain in semipolar and nonpolar InGaN/GaN laser diodes. *Phys. Rev. B* **2009**, *80*, 115320. [CrossRef]
12. Waltereit, P.; Brandt, O.; Trampert, A.; Grahn, H.T.; Menniger, J.; Ramsteiner, M.; Reiche, M.; Ploog, K.H. Nitride semiconductors free of electrostatic fields for efficient white light-emitting diodes. *Nature* **2000**, *406*, 865–868. [CrossRef]
13. Pasayat, S.S.; Gupta, C.; Wang, Y.; DenBaars, S.P.; Nakamura, S.; Keller, S.; Mishra, U.K. Compliant micron-sized patterned InGaN pseudo-substrates utilizing porous GaN. *Materials* **2020**, *13*, 213. [CrossRef]
14. Pasayat, S.S.; Gupta, C.; Wong, M.S.; Wang, Y.; Nakamura, S.; Denbaars, S.; Keller, S.; Mishra, U.K. Growth of strain-relaxed InGaN on micrometer-sized patterned compliant GaN pseudo-substrates. *Appl. Phys. Lett.* **2020**, *116*, 111101. [CrossRef]
15. Hestroffer, K.; Wu, F.; Li, H.; Lund, C.; Keller, S.; Speck, J.S.; Mishra, U.K. Relaxed c-plane InGaN layers for the growth of strain-reduced InGaN quantum wells. *Semicond. Sci. Technol.* **1050**, *2015*, 3015.
16. Even, A.; Laval, G.; LeDoux, O.; Ferret, P.; Sotta, D.; Guiot, E.; Levy, F.; Robin, I.C.; Dussaigne, A. Enhanced In incorporation in full InGaN heterostructure grown on relaxed InGaN pseudo-substrate. *Appl. Phys. Lett.* **2017**, *110*, 262103. [CrossRef]
17. White, R.C.; Li, H.; Khoury, M.; Lynsky, C.; Iza, M.; Keller, S.; Sotta, D.; Nakamura, S.; DenBaars, S.P. InGaN-Based microLED Devices Approaching 1% EQE with Red 609 nm Electroluminescence on Semi-Relaxed Substrates. *Crystals* **2021**, *11*, 1364. [CrossRef]
18. Keller, S.; Lund, C.; Whyland, T.; Hu, Y.; Neufeld, C.; Chan, S.; Wienecke, S.; Wu, F.; Nakamura, S.; Speck, J.S.; et al. InGaN lattice constant engineering via growth on (In, Ga) N/GaN nanostripe arrays. *Semicond. Sci. Technol.* **2015**, *30*, 105020. [CrossRef]
19. Chan, P.; DenBaars, S.P.; Nakamura, S. Growth of highly relaxed InGaN pseudo-substrates over full 2-in. wafers. *Appl. Phys. Lett.* **2021**, *119*, 131106. [CrossRef]
20. Chan, P.; Rienzi, V.; Lim, N.; Chang, H.M.; Gordon, M.; DenBaars, S.P.; Nakamura, S. Demonstration of relaxed InGaN-based red LEDs grown with high active region temperature. *Appl. Phys. Express* **2021**, *14*, 101002. [CrossRef]
21. Wong, M.S.; Chan, P.; Lim, N.; Zhang, H.; White, R.C.; Speck, J.S.; Denbaars, S.P.; Nakamura, S. Low Forward Voltage III-Nitride Red Micro-Light-Emitting Diodes on a Strain Relaxed Template with an InGaN Decomposition Layer. *Crystals* **2022**, *12*, 721. [CrossRef]
22. Chang, H.-M.; Chan, P.; Lim, N.; Rienzi, V.; Gordon, M.J.; DenBaars, S.P.; Nakamura, S. Demonstration of C-Plane InGaN-Based Blue Laser Diodes Grown on Strain Relaxed Template. *Crystals* **2022**, *12*, 1208. [CrossRef]
23. Nagahama, S.-I.; Iwasa, N.; Senoh, M.; Matsushita, T.; Sugimoto, Y.; Kiyoku, H.; Kozaki, T.; Sano, M.; Matsumura, H.; Umemoto, H.; et al. High-power and long-lifetime InGaN multi-quantum-well laser diodes grown on low-dislocation-density GaN substrates. *Jpn. J. Appl. Phys.* **2000**, *39*, L647. [CrossRef]
24. White, R.C.; Khoury, M.; Wu, F.; Keller, S.; Rozhavskaia, M.; Sotta, D.; Nakamura, S.; DenBaars, S.P. MOCVD growth of thick V-pit-free InGaN films on semi-relaxed InGaN substrates. *Semicond. Sci. Technol.* **2020**, *36*, 015011. [CrossRef]
25. Mehari, S.; Cohen, D.A.; Becerra, D.L.; Nakamura, S.; Denbaars, S. Demonstration of enhanced continuous-wave operation of blue laser diodes on a semipolar 202¯ 1¯ GaN substrate using indium-tin-oxide/thin-p-GaN cladding layers. *Opt. Express* **2018**, *26*, 1564–1572. [CrossRef] [PubMed]
26. Kuritzky, L.Y.; Becerra, D.L.; Abbas, A.S.; Nedy, J.; Nakamura, S.; Denbaars, S.; A Cohen, D. Chemically assisted ion beam etching of laser diode facets on nonpolar and semipolar orientations of GaN. *Semicond. Sci. Technol.* **2016**, *31*, 075008. [CrossRef]
27. Blood, P.; Lewis, G.; Smowton, P.M.; Summers, H.; Thomson, J.; Lutti, J. Characterization of semiconductor laser gain media by the segmented contact method. *IEEE J. Sel. Top. Quantum Electron.* **2003**, *9*, 1275–1282. [CrossRef]
28. Li, H.; Li, P.; Zhang, H.; Nakamura, S.; DenBaars, S.P. Demonstration of Efficient Semipolar 410 nm Violet Laser Diodes Heteroepitaxially Grown on High-Quality Low-Cost GaN/Sapphire Substrates. *ACS Appl. Electron. Mater.* **2020**, *2*, 1874–1879. [CrossRef]
29. Huang, C.Y.; Lin, Y.D.; Tyagi, A.; Chakraborty, A.; Ohta, H.; Speck, J.S.; DenBaars, S.P.; Nakamura, S. Optical waveguide simulations for the optimization of InGaN-based green laser diodes. *J. Appl. Phys.* **2010**, *107*, 023101. [CrossRef]
30. Rienzi, V.; Smith, J.; Lim, N.; Chang, H.-M.; Chan, P.; Wong, M.S.; Gordon, M.J.; DenBaars, S.P.; Nakamura, S. Demonstration of III-Nitride Red LEDs on Si Substrates via Strain-Relaxed Template by InGaN Decomposition Layer. *Crystals* **2022**, *12*, 1144. [CrossRef]

31. Cantu, P.; Wu, F.; Waltereit, P.; Keller, S.; Romanov, A.E.; DenBaars, S.P.; Speck, J.S. Role of inclined threading dislocations in stress relaxation in mismatched layers. *J. Appl. Phys.* **2005**, *97*, 103534. [CrossRef]
32. Cantu, P.; Wu, F.; Waltereit, P.; Keller, S.; Romanov, A.E.; Mishra, U.K.; DenBaars, S.P.; Speck, J.S. Si doping effect on strain reduction in compressively strained $Al_{0.49}$ $Ga_{0.51}$ N thin films. *Appl. Phys. Lett.* **2003**, *83*, 674–676. [CrossRef]
33. Romanov, A.E.; Beltz, G.E.; Cantu, P.; Wu, F.; Keller, S.; DenBaars, S.P.; Speck, J.S. Cracking of III-nitride layers with strain gradients. *Appl. Phys. Lett.* **2006**, *89*, 161922. [CrossRef]
34. Coldren, L.A.; Corzine, S.W.; Mašanović, M.L. *Diode Lasers and Photonic Integrated Circuits*; John Wiley & Sons: New York, NY, USA, 2012.